

Highly Anisotropic Thermal Conductivity of Arsenene: An *ab initio* Study

M. Zeraati^a, S. M. Vaez Allaei^{a,b}, I. Abdolhosseini Sarsari^c, M. Pourfath^{d,e}, and D. Donadio^{f,g,h,i}

a) Department of Physics, University of Tehran, Tehran 14395-547, Iran

*b)*School of Physics, Institute for Research in Fundamental Sciences (IPM), Tehran 19395-5531, Iran

*c)*Department of Physics, Isfahan University of Technology, Isfahan, 84156-83111, Iran

*d)*School of Electrical and Computer Engineering, University of Tehran, Tehran 14395-515, Iran

*e)*Institute for Microelectronics, TU Wien, Gußhausstraße 27–29/E360, 1040 Vienna, Austria

*f)*Department of Chemistry, University of California Davis, One Shields Ave. Davis, CA, 95616

*g)*Max Planck Institut für Polymerforschung, Ackermannweg 10, D-55128 Mainz, Germany

*h)*Donostia International Physics Center, Paseo Manuel de Lardizabal, 4, 20018 Donostia-San Sebastian, Spain

*i)*IKERBASQUE, Basque Foundation for Science, E-48011 Bilbao, Spain

(Dated: August 11, 2015)

Elemental 2D materials exhibit intriguing heat transport and phononic properties. Here we have investigated the lattice thermal conductivity of newly proposed arsenene, the 2D honeycomb structure of arsenic, using *ab initio* calculations. Solving the Boltzmann transport equation for phonons, we predict a highly anisotropic thermal conductivity, of 30.4 and 7.8 W/mK along the zigzag and armchair directions, respectively at room temperature. Our calculations reveal that phonons with mean free paths between 20 nm and 1 μ m provide the main contribution to the large thermal conductivity in the zig-zag direction, mean free paths of phonons contributing to heat transport in the armchair directions range between 20 and 100 nm. The obtained low and anisotropic thermal conductivity, and feasibility of synthesis, in addition to other reports on high electron mobility, make arsenene a promising material for a variety of applications, including thermal management and thermoelectric devices.

PACS numbers:

The discovery of graphene as a stable atomically thin material has led to extensive investigation of similar 2D systems. Its properties such as high electron mobility¹, and very high thermal conductivity^{2–5} make graphene very appealing for applications in electronics, for packaging and thermal management^{6–11}. The successful isolation of single-layer graphene fostered the search for further ultra-thin 2D structures, such as silicene, germanene, phosphorene, and transition metal dichalcogenides, e.g. MoS₂ and WS₂^{12,13}. These materials are now considered for various practical usages due to their distinguished properties stemming from their low dimensionality. Thermal transport in 2D materials has recently attracted the attention of the scientific community, as anomalous heat conduction has been predicted to occur in systems with reduced dimensionality¹⁴. Phononic properties and thermal conductivity vary significantly from one 2D system to another^{15–18}. For example, silicene has a buckled structure and a lower thermal conductivity^{19,20} compared to graphene^{12,21,22}.

2D structures of arsenic and phosphorous have been recently investigated^{23–27}. Arsenic and phosphorus are in the 5th group of the periodic table and both have different allotropes. Black phosphorus is a layered allotrope of phosphorus similar to graphite, and the stability of its single layer form, named *phosphorene* has been probed both theoretically and experimentally^{13,28}. *Gray arsenic* is one of the most stable allotropes of arsenic with a buckled layered structure^{27,29}. In addition, arsenic has an orthorhombic phase (puckered) similar to black phosphorus^{23,25,26}, and its monolayer is called *arsenene* (see Fig. 1). Experimental observations have shown that gray

arsenic undergoes a structural phase transition to the orthorhombic precursor of arsenene at temperatures of about $T = 370$ K³⁰. As a monolayer arsenene has a direct band gap as opposed to the multilayer allotrope, which exhibits an indirect band gap of the order of 1 eV²⁶. According to our calculations, monolayer of arsenene is stable also near zero temperature, in agreement with previous reports^{23,25,26}. Here we investigate heat conduction in arsenene and we elucidate the anisotropy of its thermal conductivity. Since in semiconductors phonons are the predominant heat carriers, we use first-principles anharmonic lattice dynamics calculations and the Boltzmann transport equation to compute phonon dispersion relations and thermal conductivity.

We employ density functional theory as implemented in the VASP code³¹ with projector-augmented-wave (PAW)³² pseudopotentials and the Perdew-Burke-Ernzerhof (PBE) generalized gradient functional³³ exchange-correlation functional. Integration over Brillouin zone is performed using $15 \times 15 \times 1$ Γ -center Monkhorst-Pack mesh of k-points³⁴ and plane waves up to an energy cutoff of 360 eV are used as basis set to represent the Kohn-Sham wave functions. The simulation cell is built with a vacuum layer of 10 Å, which is sufficient to avoid interactions between periodic images. The structural relaxations were performed by using the conjugate-gradient (CG) algorithm with a convergence criterion of 10^{-6} eV/Å for the maximum residual force component per atom.

As shown in Fig. 1, arsenene has a puckered structure arranged in a rectangular unit cell with lattice vectors $a = 3.686$ Å and $b = 4.769$ Å. The bond length between

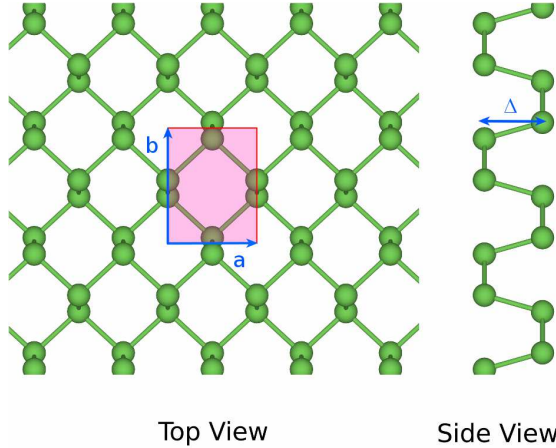


FIG. 1: Top and side view of puckered arsenene.

TABLE I: The lattice parameters of arsenene. a and b are the lattice vectors, Δ is the puckering distance, c_1 is the bond length between atoms that are in the same plane, c_2 is the bond length between atoms that are in different planes.

Mono-layer of arsenene					
Method	a (Å)	b (Å)	Δ (Å)	c_1 (Å)	c_2 (Å)
PBE	3.686	4.769	2.402	2.510	2.496
PBE (Ref. ²³)	3.677	4.765	—	2.521	2.485
revPBE-vdW (Ref. ²⁶)	3.68	4.80	—	2.51	2.49

atoms in the same plane (upper panel or lower) is 2.510 Å, while the bonding length between atoms in different planes is 2.496 Å. The distance between the two planes is denoted by Δ and is 2.402 Å. Our structural parameters are compared with previous studies in Table I. We have utilized the PHONOPY package³⁵ interfaced with VASP to compute inter-atomic force constants (IFCs). After testing convergence of the phonon frequencies as a function of the size of the supercell, a $8 \times 8 \times 1$ super-cell has been adopted, with a $3 \times 3 \times 1$ Γ-center Monkhorst-Pack mesh of k-points, to build the dynamical matrix \mathcal{D} . The frequencies of the vibrational modes are obtained by diagonalizing \mathcal{D} , and the phonon dispersion curves are represented in Fig. 2. The absence of phonon branches with negative phonon frequencies indicates the stability of the system at zero temperature.

The phonon bands exhibit two acoustic modes, a longitudinal one (LA) and an in-plane transverse one (TA), with linear dispersion ($\omega \propto q$) for $q \rightarrow 0$, and an out-of-plane flexure mode (ZA) with quadratic dispersion in the long wavelength limit, which is a general feature of 2D membranes³⁶ and have been characterized in graphene^{15,37}, silicene^{16,38}, hBN³⁹, MoS₂⁴⁰ and ultra-thin silicon membranes^{41,42}. Flexural modes have a major role in contributing to the thermal conductivity of graphene, both as carriers¹⁵ and as scatterers⁴³. In addition, we observe a gap of about 2 THz between the

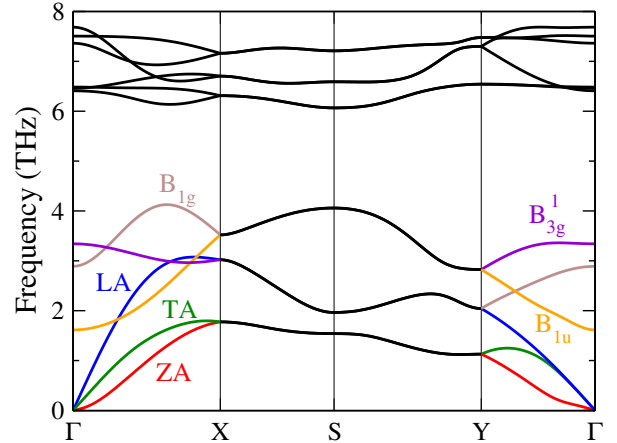


FIG. 2: (a) Phonon dispersion curves along the high-symmetry directions of the first Brillouin zone for puckered arsenene.

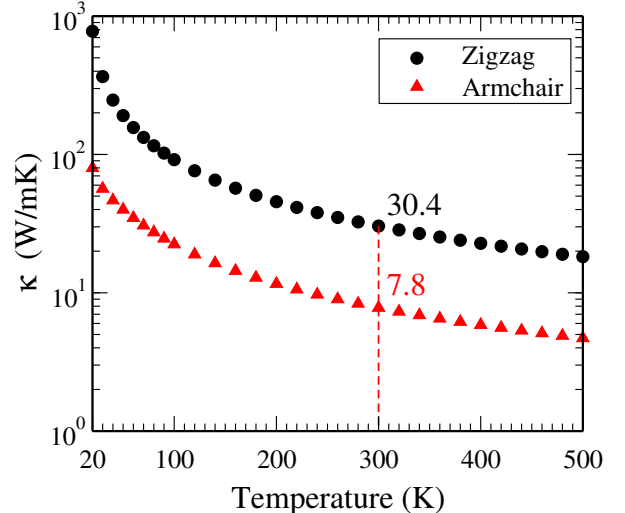


FIG. 3: The thermal conductivity of arsenene as a function of temperature along the zigzag and armchair direction.

low-frequency and high-frequency optical branches.

We have computed the thermal conductivity of arsenene by solving the phonon Boltzmann transport equation (BTE) with an iterative self-consistent algorithm^{44,45}, using the ShengBTE package⁴⁶. In our calculations we have considered third-order interatomic force constants up to the forth shell of neighbors in a $5 \times 5 \times 1$ super-cell with a $3 \times 3 \times 1$, Γ-centered Monkhorst-Pack mesh of k-points^{46,47}. Intrinsic three phonon scattering processes have been considered in the calculation of phonon relaxation times:

$$\frac{1}{\tau_\lambda^0} = \frac{1}{N} \left(\sum_{\lambda' \lambda''}^+ \Gamma_{\lambda \lambda' \lambda''}^+ + \frac{1}{2} \sum_{\lambda' \lambda''}^- \Gamma_{\lambda \lambda' \lambda''}^- + \sum_{\lambda'} \Gamma_{\lambda \lambda'}^{\text{ext}} \right), \quad (1)$$

where $\Gamma_{\lambda \lambda' \lambda''}^+$ and $\Gamma_{\lambda \lambda' \lambda''}^-$ represent the scattering rates due to absorbing and emitting three-phonon processes,

TABLE II: Sound velocity (group velocity) of acoustic modes of arsenene close to the zone center (Γ -point). (*) Due to quadratic form of ZA mode near Γ point, the magnitude has been averaged over a small reigon interval.

Sound velocity km/s			
	Arsenene	Phosphorene	
	ZA (*)	TA	LA
Armchair	0.72	2.41	2.44
Zigzag	0.34	2.41	4.77
			4.17
			7.73

respectively. The extrinsic scattering term $\Gamma_{\lambda\lambda'}^{\text{ext}}$ is zero in our calculations, since arsenic does not present isotopic disorder, and neither defect or boundary scattering processes were considered. Knowing the distribution function, the phononic thermal conductivity tensor (κ) is expressed as:

$$\kappa_{\alpha\beta} = \frac{1}{V} \sum_{\lambda} \hbar \omega_{\lambda} \frac{\partial f}{\partial T} v_{\lambda}^{\alpha} v_{\lambda}^{\beta} \tau_{\lambda}, \quad (2)$$

where f is the phonon distribution function, ω_{λ} is the phonon angular frequency, v_{λ}^{α} is the velocity component along the α -direction, and τ_{λ} is the phonon relaxation time.

The two diagonal components of the thermal conductivity at temperatures between 20 and 500 K are reported in Fig. 3. The thermal conductivity along the zigzag and armchair direction at $T = 300$ K is 30.4 and 7.8 $\text{Wm}^{-1}\text{K}^{-1}$, respectively. The nearly 3-fold ratio between the two components indicates a high anisotropy. The thermal conductivity of arsenene in comparison to graphene and hexagonal boron nitride is very low: for example both experimental and theoretical studies indicate the intrinsic thermal conductivity of graphene is larger than 3000 W/mK ^{2,3}. Due to the larger atomic weight of As, κ of arsenene is also lower than that of phosphorene, which is also strongly anisotropic, theoretically predicted as 110 and 36 $\text{Wm}^{-1}\text{K}^{-1}$ in the zigzag and armchair directions, respectively¹⁸. We note indeed that the group velocity of the acoustic modes of arsenene along both zigzag and armchair directions near the zone center are about twice as smaller as those of phosphorene (see Table II). Since according to Equation 2 group velocities contribute to κ quadratically, we can argue that the smaller v_{λ} is responsible for the difference between the thermal conductivities of arsenene and phosphorene.

The contribution of each phonon mode to the total thermal conductivity as a function of temperature is shown in Fig. 4. The ZA mode provides the largest contribution to thermal conductivity along both directions at low temperatures. However, this contribution decreases as the temperature increases and reaches 7.8% (armchair direction) for temperatures above 300 K. This is in contrast to the case of graphene where the ZA modes provide the main contribution to heat conduction¹⁵. Due to the special selection rules of phonon scattering in

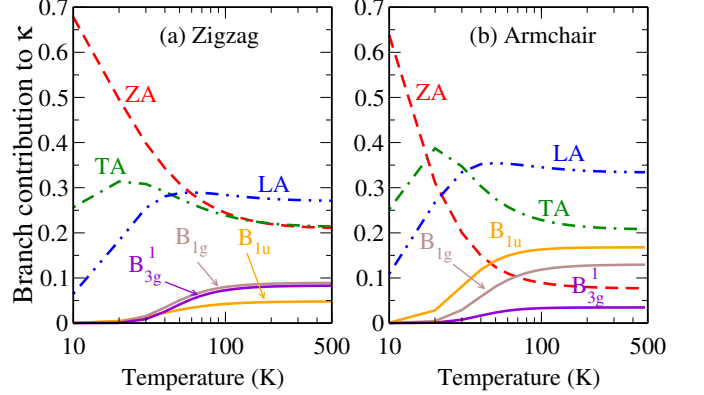


FIG. 4: Normalized contribution of each phonon branch to the total thermal conductivity, as a function of temperature along the (a) zigzag and (b) armchair directions.

graphene, the ZA mode has a relatively large relaxation time compared to other phonon modes¹⁵, while due to the puckered structure of arsenene, similar to silicene and phosphorene^{16,18}, the hexagonal symmetry of graphene is broken, resulting in larger scattering rates and shorter relaxation times of the ZA modes at high temperatures. The contribution of the ZA modes remains however substantial and roughly equivalent to that of the TA modes in the zigzag direction, while it drops below 10% in the armchair direction.

At temperatures higher than 100 K, the contribution of LA modes to the thermal conductivity is the largest in both directions. The group velocity of LA mode near the zone center is the largest along the zigzag direction, while it is comparable to the TA mode along the armchair direction (see Table II). Furthermore, the relaxation times of the LA modes at low frequencies, which play a significant role in the process of heat conduction, are larger than that of other acoustic modes (see Fig. 5). All these effects combined together result in a larger contribution of LA modes to the thermal conductivity at high temperatures.

Finally we computed the cumulative thermal conductivity as a function of phonon mean free path, defined as

$$\kappa_l(\Lambda \leq \Lambda_{\max}) = \frac{\kappa_l}{1 + \frac{\Lambda_0}{\Lambda_{\max}}}, \quad (3)$$

where Λ_{\max} is the maximum mean free path and Λ_0 is a fitting parameter that can be interpreted as the mean free path of heat-carrying phonons of infinite system size. By fitting Eq.(3) to the calculated values one can evaluate Λ_0 , see Fig. 6. This quantity shows which mean free paths contribute the most to the thermal conductivity. Phonon modes with mean free paths larger than 59.5 nm along the armchair direction and 91.8 nm along the zigzag direction have 50% contribution to the total thermal conductivity. Hence we can argue that in a polycrystalline structure with a grain size of the order of

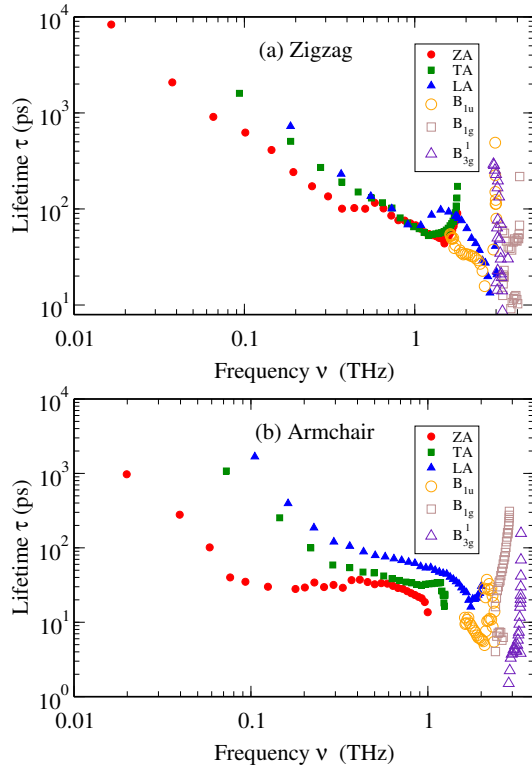


FIG. 5: Total relaxation time of phonon modes as a function of frequency ν along the (a) zigzag and (b) armchair direction.

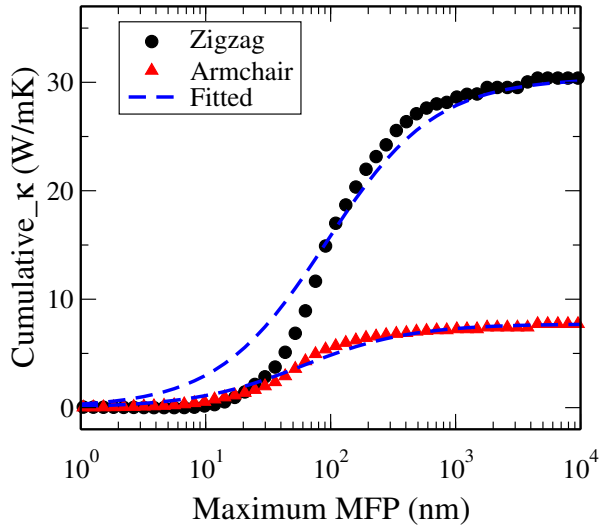


FIG. 6: Cumulative thermal conductivity of arsenene as a function of the phonon mean free path at $T = 300$ K along the zigzag and armchair directions.

50 nm the thermal conductivity can be significantly further reduced. However, given the broad range of mean free paths that contribute, the most efficient approach to abate κ would be hierarchical nanostructuring⁴⁹.

In summary we have theoretically investigated the phonon properties and the thermal conductivity of arsenene by *ab initio* anharmonic lattice dynamics. Our calculations evidence the lowest thermal conductivity among the 2D elemental materials found so far. The larger mass of arsenic atoms compared to phosphorus leads to a 3 times smaller thermal conductivity of this material compared to phosphorene. Similar to phosphorene, the thermal conductivity of arsenene is strongly anisotropic. Such anisotropy could be utilized in thermal engineering application, to establish directional heat transport at the nanoscale. Unlike graphene, the longitudinal acoustic phonon modes provide the main contribution to the thermal conductivity of arsenene at temperatures above 100 K, which is mainly due to the puckered structure of this material. From this observation, we expect that κ of arsenene would be less affected by the interaction with a substrate than in those materials for which the main contribution comes from flexural modes. In addition, given the high electron mobility and the reduced dimensionality, which should enhance the Seebeck coefficient, its relatively low and strongly directional thermal conductivity makes arsenene a good candidate from thermoelectric energy conversion.

The work of S.M.V.A. was supported in part by the Research Council of the University of Tehran.

¹ K. S. Novoselov, a. K. Geim, S. V. Morozov, D. Jiang, M. I. Katsnelson, I. V. Grigorieva, S. V. Dubonos, and a. a. Firsov, Nature **438**, 197 (2005), ISSN 1476-4687.

² X. Xu, L. F. C. Pereira, Y. Wang, J. Wu, K. Zhang, X. Zhao, S. Bae, C. Tinh Bui, R. Xie, J. T. L. Thong,

et al., Nat Commun **5** (2014).

³ G. Fugallo, A. Cepellotti, L. Paulatto, M. Lazzeri, N. Marzari, and F. Mauri, Nano letters (2014), ISSN 1530-6992.

⁴ L. Lindsay, W. Li, J. Carrete, N. Mingo, D. A. Broido, and

- T. L. Reinecke, Phys Rev B **89**, 155426 (2014).
- ⁵ A. Cepellotti, G. Fugallo, L. Paulatto, M. Lazzeri, F. Mauri, and N. Marzari, Nature Communications **6**, 6400 (2015).
- ⁶ P. Wei, W. Bao, Y. Pu, C. N. Lau, and J. Shi, Phys. Rev. Lett. **102**, 166808 (2009), ISSN 0031-9007.
- ⁷ Y. M. Zuev, W. Chang, and P. Kim, Phys. Rev. Lett. **102**, 096807 (2009), ISSN 0031-9007.
- ⁸ C.-R. Wang, W.-S. Lu, L. Hao, W.-L. Lee, T.-K. Lee, F. Lin, I.-C. Cheng, and J.-Z. Chen, Phys. Rev. Lett. **107**, 186602 (2011), ISSN 0031-9007.
- ⁹ A. Rajabpour, S. M. Vaez Allaei, and F. Kowsary, Appl. Phys. Lett. **99**, 2011 (2011), ISSN 00036951.
- ¹⁰ a. Rajabpour and S. M. Vaez Allaei, Appl. Phys. Lett. **101**, 053115 (2012), ISSN 00036951.
- ¹¹ Z. Yan, G. Liu, J. M. Khan, and A. A. Balandin, Nature Communications **3**, 827 (2012).
- ¹² a. K. Geim and I. V. Grigorieva, Nature **499**, 419 (2013), ISSN 1476-4687.
- ¹³ J. Guan, Z. Zhu, and D. Tománek, Phys. Rev. Lett. **113**, 046804 (2014), ISSN 0031-9007.
- ¹⁴ S. Lepri, R. Livi, and A. Politi, Phys Rep **377**, 1 (2003).
- ¹⁵ L. Lindsay, D. a. Broido, and N. Mingo, Phys. Rev. B **82**, 115427 (2010), ISSN 1098-0121.
- ¹⁶ H. Xie, M. Hu, and H. Bao, Appl. Phys. Lett. **104**, 131906 (2014), ISSN 0003-6951.
- ¹⁷ W. Li, J. Carrete, and N. Mingo, Appl. Phys. Lett. **103**, 253103 (2013), ISSN 00036951.
- ¹⁸ A. Jain and A. J. H. McGaughey, Scientific reports **5**, 8501 (2015), ISSN 2045-2322.
- ¹⁹ H. Xie, M. Hu, and H. Bao, Appl. Phys. Lett. **104**, 131906 (2014), ISSN 0003-6951.
- ²⁰ K. Yang, S. Cahangirov, A. Cantarero, A. Rubio, and R. D'Agosta, Phys. Rev. B **89**, 125403 (2014), ISSN 1098-0121.
- ²¹ L. Chen, C.-C. Liu, B. Feng, X. He, P. Cheng, Z. Ding, S. Meng, Y. Yao, and K. Wu, Physical review letters **109**, 56804 (2012).
- ²² P. Vogt, P. De Padova, C. Quaresima, J. Avila, E. Frantzeskakis, M. C. Asensio, A. Resta, B. Ealet, and G. Le Lay, Phys. Rev. Lett. **108**, 155501 (2012), ISSN 0031-9007.
- ²³ C. Kamal and M. Ezawa, Phys. Rev. B **91**, 85423 (2015).
- ²⁴ S. Zhang, Z. Yan, Y. Li, Z. Chen, and H. Zeng, Angewandte Chemie **127**, 3155 (2015), ISSN 00448249.
- ²⁵ Z. Y. Zhang, H. N. Cao, J. C. Zhang, Y. H. Wang, D. S. Xue, and M. S. Si (2015), 1501.06044.
- ²⁶ Z. Y. Zhang, J. Xie, D. Z. Yang, D. S. Xue, M. S. Si, and W. Ji, **1** (2014), 1411.3165.
- ²⁷ Z. Zhu, J. Guan, and D. Tomanek, p. 5 (2014), 1410.6371.
- ²⁸ H. Liu, A. T. Neal, Z. Zhu, Z. Luo, X. Xu, D. Tománek, and P. D. Ye, ACS nano **8**, 4033 (2014), ISSN 1936-086X.
- ²⁹ O. Madelung, *Semiconductors: Data Handbook* (Springer Berlin Heidelberg, Berlin, Heidelberg, 2004), ISBN 978-3-642-62332-5.
- ³⁰ H. Krebs, W. Holz, and K. H. Worms, Zeitschrift für Naturforschung B **12** (1957), ISSN 1865-7117.
- ³¹ G. Kresse and J. Furthmüller, Phys. Rev. B **54**, 11169 (1996).
- ³² P. E. Blöchl, Phys. Rev. B **50**, 17953 (1994), ISSN 0163-1829.
- ³³ J. P. Perdew, K. Burke, and M. Ernzerhof, Phys. Rev. Lett. **77**, 3865 (1996).
- ³⁴ H. J. Monkhorst and J. D. Pack, Phys. Rev. B **13**, 5188 (1976).
- ³⁵ A. Togo, F. Oba, and I. Tanaka, Phys. Rev. B **78**, 134106 (2008).
- ³⁶ H. Zabel, Journal of Physics: Condensed Matter **13**, 7679 (2001), ISSN 0953-8984.
- ³⁷ J.-W. Jiang, B.-S. Wang, J.-S. Wang, and H. S. Park, Journal of physics. Condensed matter : an Institute of Physics journal **27**, 083001 (2015).
- ³⁸ S. Cahangirov, M. Topsakal, E. Aktürk, H. ahin, and S. Ciraci, Phys. Rev. Lett. **102**, 236804 (2009), ISSN 0031-9007.
- ³⁹ L. Lindsay and D. a. Broido, Phys. Rev. B **84**, 155421 (2011), ISSN 1098-0121.
- ⁴⁰ Y. Cai, J. Lan, G. Zhang, and Y.-W. Zhang, Phys. Rev. B **89**, 035438 (2014), ISSN 1098-0121.
- ⁴¹ S. Neogi and D. Donadio, The European Physical Journal B **88**, 73 (2015).
- ⁴² S. Neogi, J. S. Reparaz, L. F. C. Pereira, B. Graczykowski, M. Sledzinska, A. Shchepetov, M. Prunnila, J. Ahopelto, C. M. Sotomayor-Torres, and D. Donadio, ACS Nano **9**, 3820 (2015).
- ⁴³ L. F. C. Pereira and D. Donadio, Phys. Rev. B **87**, 125424 (2013), URL <http://link.aps.org/doi/10.1103/PhysRevB.87.125424>.
- ⁴⁴ R. Peierls, Ann. Phys **3**, 1055 (1929).
- ⁴⁵ M. Omini and A. Sparavigna, Phys. Rev. B **53**, 9064 (1996).
- ⁴⁶ W. Li, J. Carrete, N. Katcho, and N. Mingo, Computer Physics Communications **185**, 1747 (2014), ISSN 00104655.
- ⁴⁷ K. Esfarjani and H. T. Stokes, Phys. Rev. B **77**, 144112 (2008), ISSN 1098-0121, URL <http://link.aps.org/doi/10.1103/PhysRevB.77.144112>.
- ⁴⁸ A. Jain and A. J. H. McGaughey, Scientific reports **5**, 8501 (2015), ISSN 2045-2322, URL <http://www.ncbi.nlm.nih.gov/pubmed/25686917>.
- ⁴⁹ K. Biswas, J. He, I. D. Blum, C.-I. Wu, T. P. Hogan, D. N. Seidman, V. P. Dravid, and M. G. Kanatzidis, Nature **489**, 414 (2012).